Supplementary Information

Computer-aided design of short peptide ligands targeting N-formyl peptide MT-ND6：potential application in treating severe inflammatory diseases

Wenhui Zong,#[a] Zhuang Liu,#[b] Zibo Yang,[a] Lin Cheng,[a] Mengrou Shi,[a] Guixian Zhang,[a] Xiaolin Wang,[a] Jian Chen,[c] Xiaohui Wang,*[a] Lailiang Ou*[b] and Wenzhong Li*[d]

[a] Department of Medical Biomaterials, Tianjin Institute of Medical and Pharmaceutical Sciences, Tianjin Medicine and Health Research Center, Tianjin 300020, China

Email: wangtxh@126.com

[b] Key Laboratory of Bioactive Materials, Ministry of Education, College of Life Science, Nankai University, Tianjin 300071, China.

Email: ouyll@nankai.edu.cn

[c] Fujian Key Laboratory of Molecular Neurology, Institute of Neuroscience, Fujian Medical University, Fuzhou 350004, China.

[d] School of Ophthalmology & Optometry, Eye Hospital, School of

Biomedical Engineering, Wenzhou Medical University, Wenzhou, Zhejiang, 325027, China.

Email: bcrtlwz@gmail.com

Corresponding author: (E-mail: wangtxh@126.com, ouyll@nankai.edu.cn, bcrtlwz@gmail.com)

Table S1

The peptide ligand sequences and their binding energies for MT-ND6

（The yellow ones are three peptides in the main text）

Name	Energy(kcal/mol)	Amino acid sequence
out_205_6_204.log:	-7.6	RFVIGF（RF）
out_205_7_203.log:	-7.6	IRFVIGF
out_106_6_104.log:	-7.5	VDINLF(VF)
out_106_7_105.log:	-7.4	DINLFGS
out_106_7_101.log:	-7.3	HIVVDIN
out_201_7_196.log:	-7.3	MLTARGI
out_201_7_197.log:	-7.3	LTARGII
out_205_5_203.log:	-7.3	IRFVI
out_205_7_200.log:	-7.3	RGIIRFV
out_106_5_102.log:	-7.2	IVVDI
out_106_5_105.log:	-7.2	DINLF
out_106_7_104.log:	-7.2	VDINLFG
out_201_6_197.log:	-7.2	LTARGI(LI)
out_205_4_202.log:	-7.2	IIRF
out_205_7_204.log:	-7.2	RFVIGFS
out_201_5_199.log:	-7.1	ARGII
out_205_4_204.log:	-7.1	RFVI
out_205_7_199.log:	-7.1	ARGIIRF
out_106_5_104.log:	-7	VDINL
out_106_7_100.log:	-7	IHIVVDI
out_201_5_198.log:	-7	TARGI
out_205_4_203.log:	-7	IRFV
out_205_5_201.log:	-7	GIIRF
out_205_6_203.log:	-7	IRFVIG

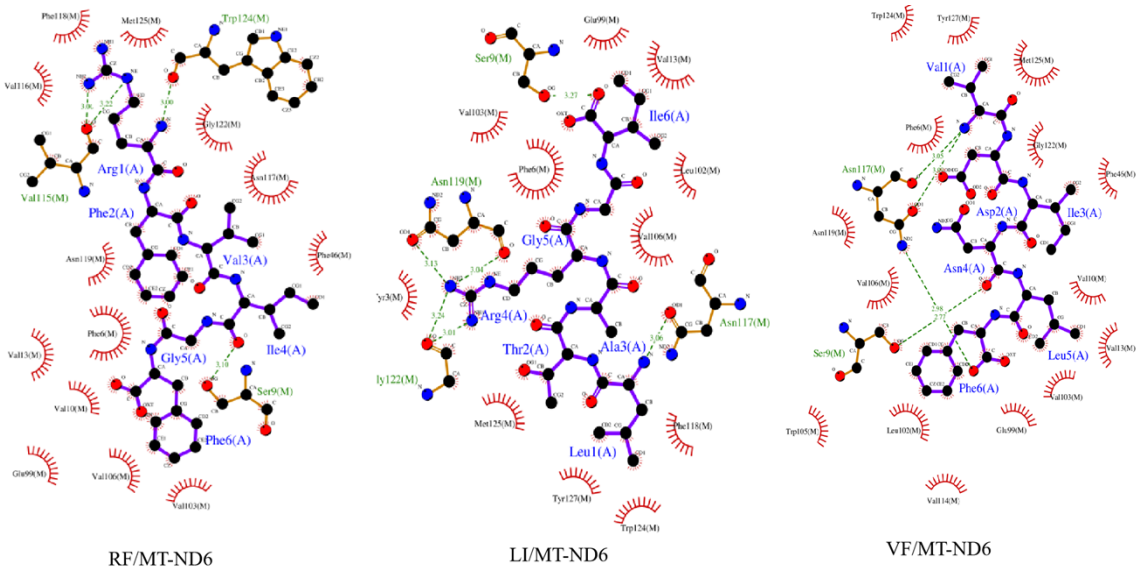

Figure S1 2D interaction between peptides and MT-ND6 by LigPlus

LigPlus shows:

RFVIGF forms hydrogen bonds with residues TRP124, SER9, and VAL115, and exhibits non-covalent interactions(including Van Der Waals force and electrostatic interaction) with hydrophobic residues PHE118, VAL116, PHE6, VAL13, VAL10, VAL106, VAL103, PHE46, and MET125, hydrophilic residues ASN119, GLU99, and ASN117, and neutral residue GLY122.

VDINLF forms hydrogen bonds with residues ASN117 and SER9, and has non-covalent interactions with hydrophobic residues TRP124, TYR127, MET125, PHE46, VAL10, VAL13, VAL103, VAL114, LEU102, TRP105, VAL106, PHE6, hydrophilic residues GLU99 and ASN119, and neutral residue GLY122.

LTARGI forms hydrogen bonds with residues ASN119, GLY122, and ASN117, and has non-covalent interactions with hydrophobic residues VAL13, LEU102, VAL106, PHE118, TRP124, TYR127, MET125, TYR3, PHE6, and VAL103, as well as hydrophilic residue GLU99.

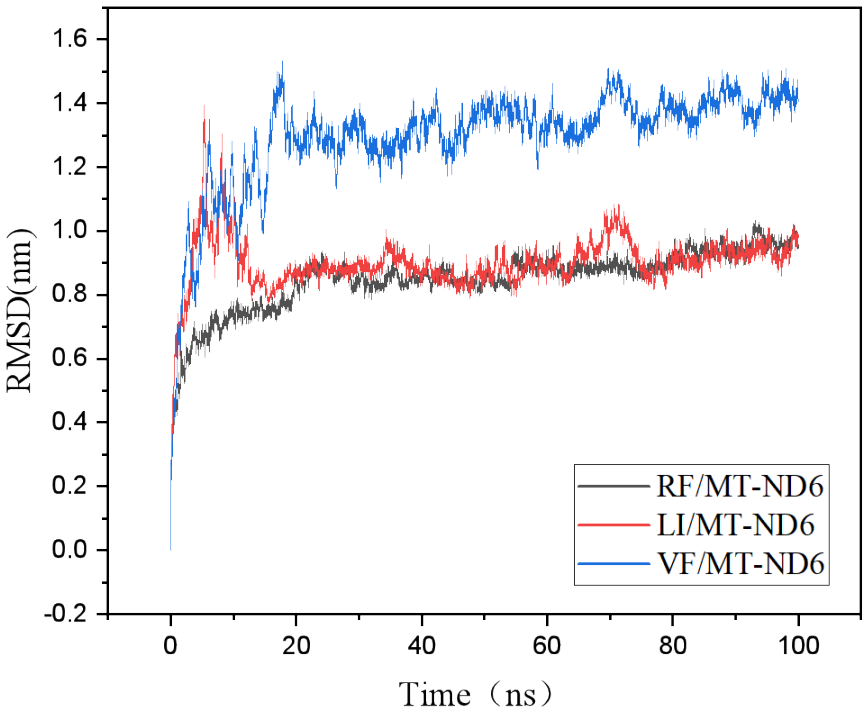

Figure S2. RMSD plots of MT-ND6 and peptides complex during 100ns MD simulation

To find out time-dependent conformational modication and the stability of complexes, RMSD analysis was undertaken. The RMSD of each peptide and the MT-ND6 complex was performed and are presented in Fig. S2. The RMSD value of MT-ND6 associated with the peptide LI (0.9 nm) is close to that of RF/MT-ND6 complex and lower than that of VF/MT-ND6 (1.3 nm). It is worthy noting that MT-ND6/RF have the most stable RMSD value.

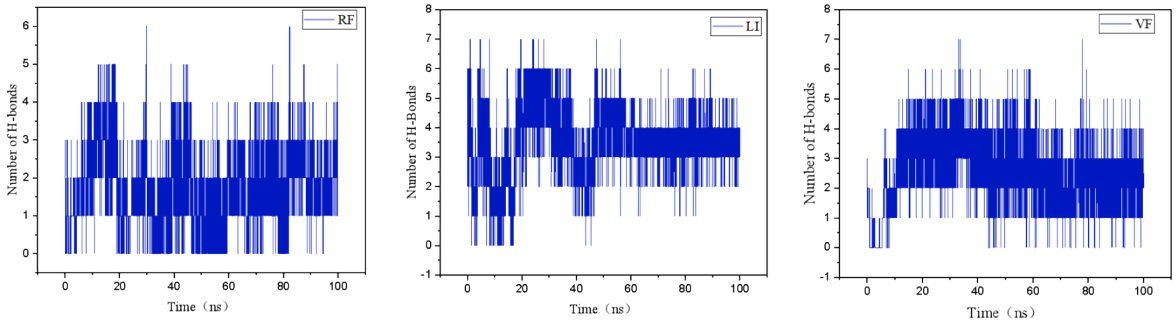

Figure S3. Number of hydrogen bonding interactions between MT-ND6 and the different peptides during 100 ns MD simulation for: RF/MT-ND6, VF/MT-ND6, LI/MT-ND6

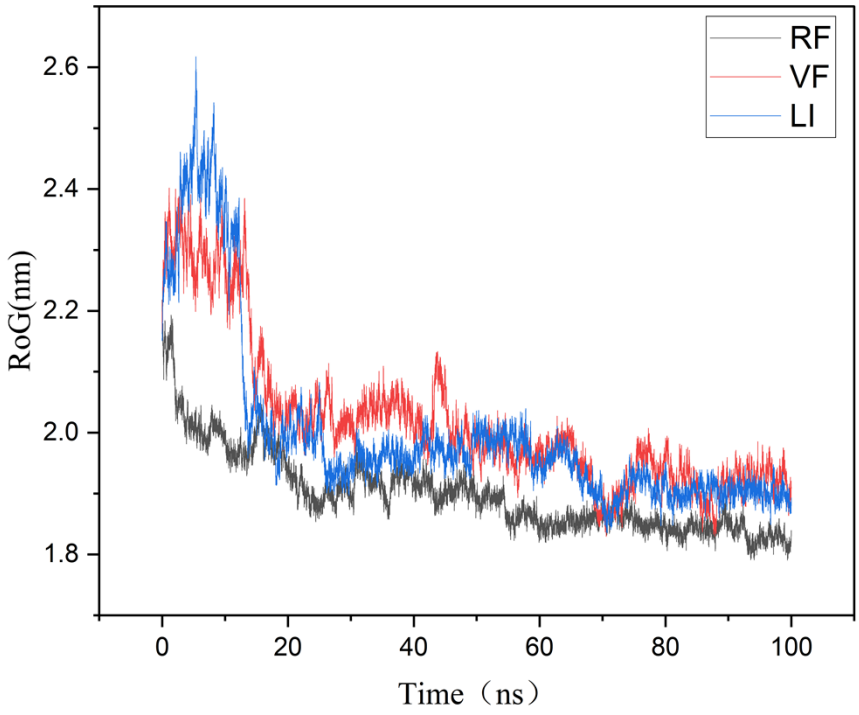

Figure S4. RoG plots of MT-ND6/peptides during simulation time

We analyzed the gyration radii which can provide information related to the folding and unfolding of the protein structure upon binding of the ligands. High RoG values would explain less compactness with high conformational entropy while low values denote high compactness and more stability of the structure. As evident from Fig. S4，the MT-ND6/RF system was more compact throughout the simulation, which indicate that the MT-ND6/RF system are better converged than the others.

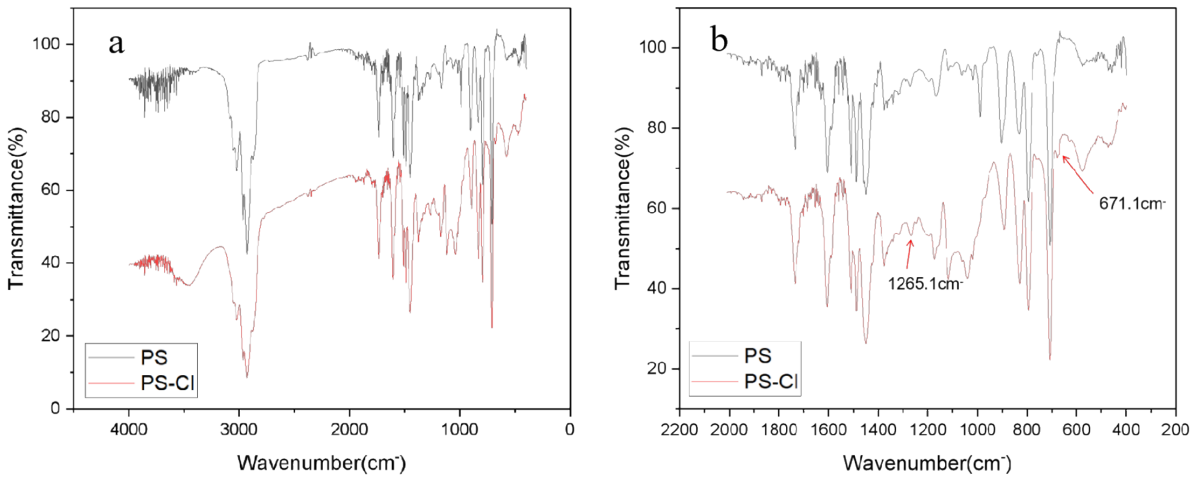

Figure S5. FT-IR spectrum of PS and PS-Cl

It is observed from Fig. S5(a), the absorption region of 3100 to 3000 cm^{-1} is related to the stretching of the Csp2-H bond of aromatic rings, 3000~2800 cm^{-1} is related to Csp3-H stretch, 1500~1400cm^{-1} is due the angular deformations from C-H bonds in the plane. These absorption bands are characteristic for PS microspheres.

As displayed in Fig. S5b, two strong representative peaks of the CH_2Cl groups at 1265.1 and 671.1 cm^{-1} are increased after chloromethylation reaction.[1-3]

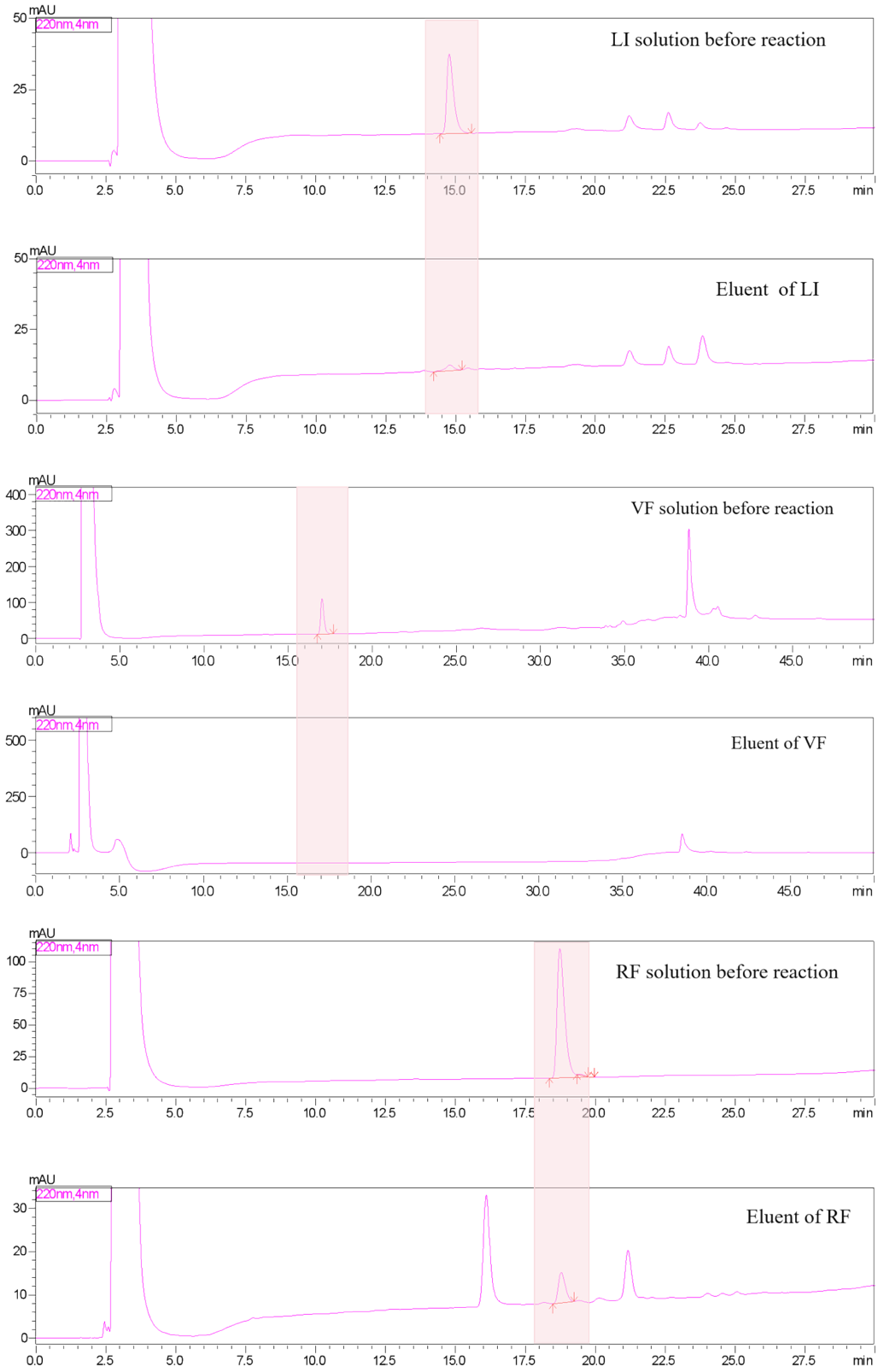

Figure S6. HPLC chromatograms

Table S2

The physical parameters of the adsorbents

Adsorbent	S_{BET}(m^2 g^{-1})	Tp (cm^3 g^{-1})	D_p(nm)
PS	593.68	1.3774	9.2805
PS-LI	515.86	0.8297	6.4336
PS-VF	512.16	0.8738	6.8246
PS-RF	521.47	0.8957	6.8703

S_{BET}: the maximum BET surface areas; T_p: the largest total pore volume; D_p: the average pore diameter.

Table S3

Adsorption kinetic constants for MT-ND6 adsorption

	$Q_{e,exp}$	Pseudo-first-order model			Pseudo-second-order model		
		$Q_{e,cal,1}$	$K_1(min^{-1})$	R_1^2	$Q_{e,cal,2}$	$K_2(g\ pg^{-1}min^{-1})$	R_2^2
PS	2993.68	2992.97	0.06605	0.9999	3405.82	2.48E-5	0.9912
PS-RF	6094.09	6042.96	0.07222	0.9906	6834.39	1.36E-5	0.9760

Cytotoxicity

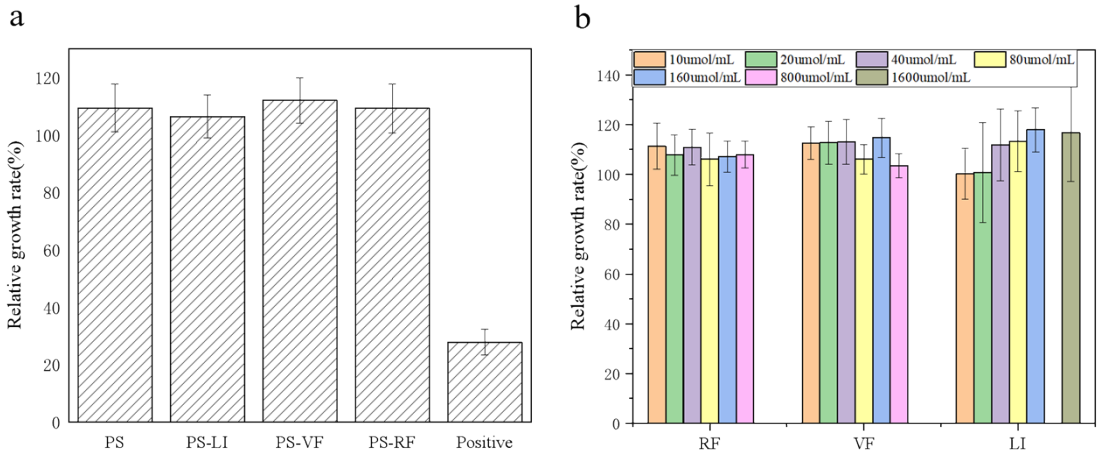

Figure S7. Cytotoxicity of different adsorbents(a) and peptides(b)

Reference：

1. C. He, J. Huang, C. Yan, J. Liu, L. Deng and K. Huang, *Journal of Hazardous Materials*, 2010, **180**, 634-639.
2. M. d. O. Reis, R. G. de Sousa and A. d. S. M. Batista, *MethodsX*, 2022, **9**, 101764.
3. L. Yang, Y. Li, L. Wang, Y. Zhang, X. Ma and Z. Ye, *Journal of Hazardous Materials*, 2010, **180**, 98-105.